ACS OMEGA

Article

http://pubs.acs.org/journal/acsodf

Magnetic Co-Doped MoS_2 Nanosheets for Efficient Catalysis of Nitroarene Reduction

C. Nethravathi, Janak Prabhu, S. Lakshmipriya, and Michael Rajamathi*

Materials Research Group, Department of Chemistry, St. Joseph's College, 36 Lalbagh Road, Bangalore 560027, India

Supporting Information

ABSTRACT: Co-doped MoS_2 nanosheets have been synthesized through the hydrothermal reaction of ammonium tetrathiomolybdate and hydrazine in the presence of cobalt acetate. These nanosheets exhibit a dominant metallic 1T phase with cobalt ion-activated defective basal planes and S-edges. In addition, the nanosheets are dispersible in polar solvents like water and methanol. With increased active sites, Co-doped MoS_2 nanosheets exhibit exceptional catalytic activity in the reduction of nitroarenes by $NaBH_4$ with impressive turnover frequencies of 8.4, 3.2, and 20.2 min^{-1} for 4-nitrophenol, 4-nitroaniline, and nitrobenzene, respectively. The catalyst is magnetic, enabling its easy separation from the reaction mixture, thus making its recycling and reusability simple and efficient. The enhanced catalytic activity of the Co-doped 1T MoS_2 nanosheets in comparison to that of undoped 1T MoS_2 nanosheets suggests that incorporation of cobalt ions in the MoS_2 lattice is the major reason for the efficiency of the catalyst. The dopant, Co, plays a dual role. In addition to providing active sites where electron transfer is assisted through redox cycling, it renders the nanosheets magnetic, enabling their easy removal from the reaction mixture.

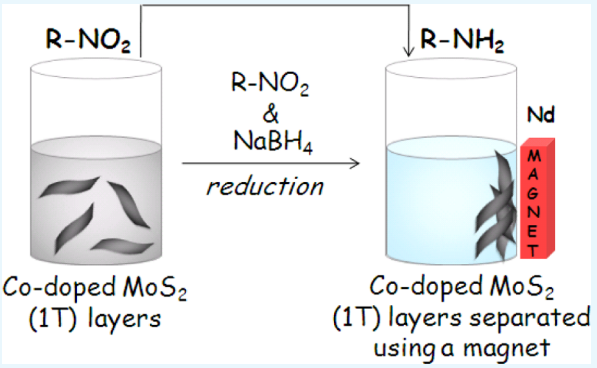

1. INTRODUCTION

Two-dimensional (2D) MoS_2 nanosheets[1] have garnered interest as a potential noble-metal-free catalyst for the electrochemical generation of hydrogen from water[2−4] and hydrodesulfurization of petroleum.[5,6] Theoretical and experimental studies indicate that the catalytic activity of the thermodynamically stable 2H polymorph of MoS_2 is associated with its metallic edges, whereas its semiconducting basal plane is catalytically inert.[2,4]

In this context, nanostructures of MoS_2, amorphous[7−9]/crystalline,[10−13] and vertically aligned structures[14,15] have been explored to maximize the number of active edge sites. MoS_2 is also hybridized with conducting/semiconducting/magnetic materials (graphene[15−19]/$CoSe_2$[20]/CoS[21−24]/CdS[25,26]/Fe_3O_4[27]) to enhance the catalytic activity through synergetic coupling effects. Metastable, intrinsically metallic, octahedral 1T MoS_2 obtained through exfoliation of trigonal prismatic 2H MoS_2 has proven to be an excellent catalyst for H_2 evolution reactions as the 1T phase facilitates electrode kinetics by increasing the electric conductivity and proliferation of the catalytic active sites.[28−30] Introducing transition metal ions (Co, Ni, Fe) into the MoS_2 matrix has been the classic route to maximize the catalytic activity of MoS_2, as the doped ions alter the electronic properties at the coordinatively unsaturated catalytic S-edges.[10,31,32] These strategies have been designed, largely, to either optimize the density of active edge sites by reducing the dimensions along the *z* direction or *xy* direction (nanostructures)[33] or increase the conductivity by stabilizing the 1T MoS_2 polytype.[19,28,29] The question is, would it be possible to tune both the structural features and electronic properties simultaneously to increase the catalytic active sites? Doping 2H MoS_2 with Co has been shown to increase its catalytic efficiency through increased active sites in the basal planes in addition to edges.[34] It would be of interest to prepare Co-doped 1T MoS_2 because in addition to all of the above effects, there would be increased conductivity.

One of the standard reactions to test the electron transfer catalytic action is the reduction of nitroarenes by $NaBH_4$. Nitroarenes, with aromatic rings associated with H-bonding $-NH_2$ and $-OH$ groups, enable the reduction to be carried out in water, making it a green reaction. This study demonstrates a single-step robust strategy to synthesizing 1T Co-doped MoS_2 nanosheets. With increased active sites, Co-doped MoS_2 nanosheets exhibit exceptional catalytic activity in the reduction of nitroarenes. The observed turnover frequency (TOF) is far superior in comparison to that of other MoS_2 architectures and noble-metal-based catalysts, reported so far.

2. RESULTS AND DISCUSSION

The XRD pattern of as-prepared Co-doped MoS_2 nanosheets (Figure 1A,a) exhibits a broad 002 reflection at 11.0 Å, indicating the presence of guest species in the interlayer.[35,36]

Received: June 23, 2017
Accepted: August 30, 2017
Published: September 18, 2017

DOI: 10.1021/acsomega.7b00848
ACS Omega 2017, 2, 5891−5897

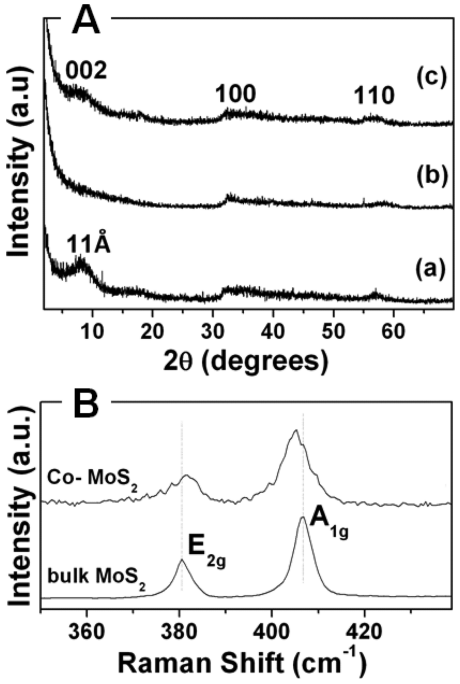

Figure 1. (A) XRD patterns of Co-doped MoS_2 nanosheets (a) as-prepared and (b) treated with 1 N HCl and of (c) MoS_2 prepared in the absence of cobalt. (B) Raman spectrum of Co-doped MoS_2 nanosheets in comparison with bulk MoS_2.

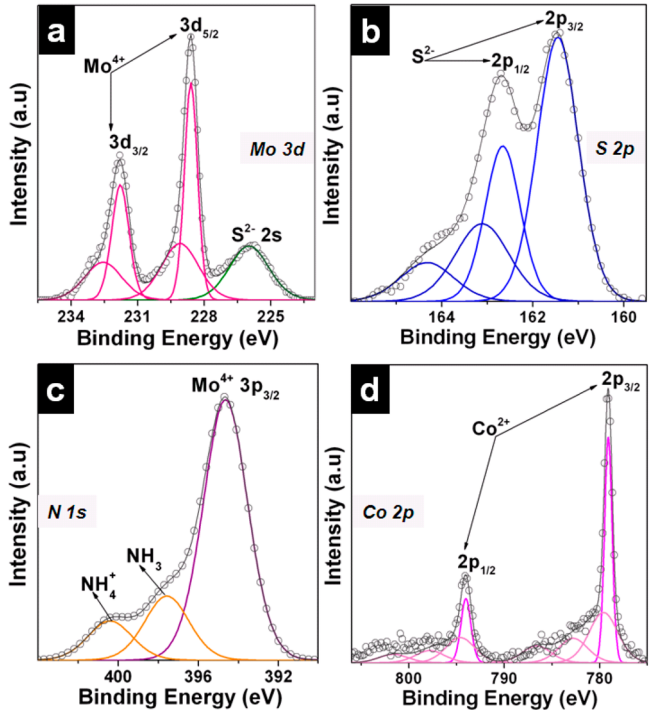

Figure 2. XPS spectra showing Mo 3d (a), S 2p (b), N 1s (c), and Co 2p (d) core-level peak regions of Co-doped MoS_2.

The guest entity could possibly be NH_3/NH_4^+ ions released as byproducts of hydrazine used as a reductant in the hydrothermal reaction.

On treating Co-doped MoS_2 nanosheets with 1 N HCl solution, the 002 reflection (Figure 1A,b) disappears, indicating deintercalation of the guest species. However, the low intensity of the 002 reflection or its absence (Figure 1A,a,b) suggests that Co-doped MoS_2 nanosheets are poorly ordered along the stacking direction and comprise largely exfoliated layers. The asymmetric 2D reflections at 2θ = 33 and 57° reveal the presence of stacking faults[37,38] within the few-layered Co-doped MoS_2. The undoped MoS_2 is also poorly ordered and exhibits increased basal spacing due to NH_3/NH_4^+ intercalation (Figure 1A,c).

The Raman spectrum of Co-doped MoS_2 (Figure 1B) exhibits the in-plane E_{2g} (380 cm^{-1}) and out-of-plane A_{1g} (406 cm^{-1}) Mo−S vibration modes, characteristic of the MoS_2 layered structure. An additional peak at 220 cm^{-1} in Figure S1 (Supporting Information, SI) indicates the presence of 1T polytype. Increased full width at half-maximum and the shift in the A_{1g} and E_{2g} modes of Co-doped MoS_2 in comparison to those of bulk MoS_2 clearly indicate softening of A_{1g} and E_{2g} modes and phonon confinement that is expected for mono- to few-layer MS_2, thus indicating that the Co-doped MoS_2 comprises mono to few layers.[39,40]

The chemical composition of the Co-doped MoS_2 was further probed by X-ray photoelectron spectroscopy (XPS). Mo 3d and S 2p spectra (Figure 2a,b; Table 1) correspond to Mo^{4+} and S^{2-} of the 1T polytype of MoS_2. A small proportion of the 2H polytype coexists with the 1T phase.[41] The N 1s spectrum (Figure 2c; Table 1) indicates the presence of NH_3 and NH_4^+ ions, which are accommodated in the interlayer of MoS_2 nanosheets, as suggested by the XRD pattern (Figure 1a).[35] The core-level Co 2p spectra (Figure 2d; Table 1) confirm the presence of Co^{2+} species. The XRD pattern (Figure 1a) and the XPS Co 2p spectra confirm the absence of CoS_2 and $CoMo_2S_4$. The binding energy of 779.2 eV is close to what has been observed for $CoMo_2S_4$, suggesting that Co^{2+} substitutes Mo atoms along the {002} or the S-edge planes of MoS_2. The atomic percentages of Co, Mo, S, and N are 4.68, 24.66, 59.38, and 11.27, respectively, leading to a chemical composition of $Co_{0.16}Mo_{0.83}S_2(NH_3)_{0.38}$.

To understand the nature of the chemical environment of Co^{2+}, the Co-doped MoS_2 was treated with 1 N HCl when the intercalated or undoped Co^{2+} species, if any, was expected to be leached out. Cobalt estimation of the leachate showed that only about 30% of the cobalt could be leached out by acid. This was further confirmed by the atomic percentages (Co-3.36, Mo-27.11, S-69.54) in the acid-leached Co-doped MoS_2 arrived at from XPS data. The composition of the acid-leached sample is $Co_{0.1}Mo_{0.78}S_2$. The XPS spectra of acid-treated Co-doped MoS_2 (SI, Figure S2) indicate that whereas the nitrogen-containing species, NH_3 and NH_4^+ ions, are absent, Co^{2+} and 1T phase of MoS_2 nanosheets are retained. These further suggest that Co^{2+} is present in the MoS_2 lattice. Hydrothermally synthesized MoS_2 has been shown to have a defective basal plane as well as unsaturated S-edges.[42] Recent studies by Liu et al.[34] demonstrate that Co^{2+} is doped at S vacancies in basal planes as well as at the unsaturated S-edges.

The magnetic hysteresis loop measured on the powder sample indicates a weak ferromagnetic behavior (Figure 3). The saturation magnetization (M_S) at 300 K of Co-doped MoS_2 nanosheets is 0.0029 emu g^{-1}, which is comparable to that of exfoliated 1T MoS_2 reported in the literature.[43] Because our control 1T MoS_2 is nonmagnetic, it is fair to assume that the magnetism in Co-doped MoS_2 arises as a consequence of doping. The magnetism in monolayer MoS_2 and its doped analogues depends on the nature of edges, type of edge defects, lattice strain, and the dopant concentration. Theoretical

DOI: 10.1021/acsomega.7b00848
ACS Omega 2017, 2, 5891−5897

Table 1. Summary of the Binding Energies of Mo, S, Co and N in Co-doped MoS_2

	binding energy (eV)				
	Mo 3d	phase	S 2p	Co 2p	N 1s
$Mo_{0.83}Co_{0.16}S_2(NH_3)_{0.38}$	228.6 & 231.8 229.0 & 232.5	1T 2H	161.49 & 162.80 163.97 & 164.77	779.2 & 794.0	397.6 – NH_3 400.4 – NH_4^+

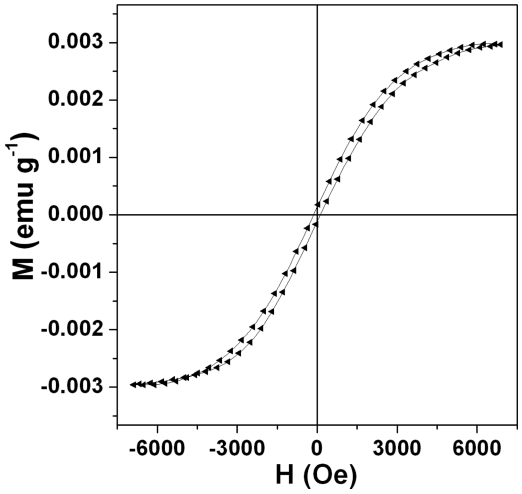

Figure 3. Hysteresis loop of the Co-doped MoS_2 nanosheets at 300 K.

calculations by Wang et al.[44] reveal that low concentrations of 4 and 6% of Co^{2+} doping in the Mo vacant sites of the basal planes result in stable magnetic moments at room temperature. Yun et al.[45] and Saab et al.[46] also reported tuning of electronic and magnetic properties due to doping of metal ions in the MoS_2 lattice. The very low M_S observed for Co-doped MoS_2 suggests that the weak ferromagnetism here originates from the strain in the layer rather than from ordering of Co^{2+} ions. Co-doped MoS_2 (Figure 3) as well as the acid-leached product is weakly magnetic, suggesting that Co^{2+} ions are doped in the MoS_2 layers. In addition, the presence of Co^{2+} in the MoS_2 lattice could be the reason for the retention of metastable 1T structure even after deintercalation of the intercalants (SI, Figure S2). All of these results indicate that Co^{2+} is possibly doped in the basal plane and S-edge planes of MoS_2 layers.

Clusters of layers are observed in the SEM image (Figure 4a) of as-synthesized Co-doped MoS_2. The bright-field transmission electron microscopy (TEM) image (Figure 4b) indicates that the transparent layers are few-layer thick and few hundred nanometers in lateral dimensions. The HRTEM image (Figure 4c) shows lattice fringes with a spacing of 1.1 nm, which correlates with the basal spacing observed in the XRD pattern (Figure 1a), suggesting the presence of intercalants. The HRTEM image in Figure 4d clearly shows that the layers are crystalline, exhibiting (100) lattice planes. Except for the circled regions representing the 2H phase, the layers largely exist as the 1T polytype.[43]

Figure 5 schematically depicts the catalytic reduction of nitroarenes. Catalytic performance of Co-doped MoS_2 in the reduction of 4-nitrophenol (4-NP) in water is summarized in Figure 6a,d–f. UV–visible absorption spectra (Figure 6a) of the reaction mixture indicate that 4-nitrophenol converts to 4-aminophenol within 7 min. The absorption peak at 400 nm is due to the nitro phenolate ion, and the intensity of this peak decreases with time and disappears completely at 7 min. Peaks at 235 and 308 nm emerge due to the formation of amino

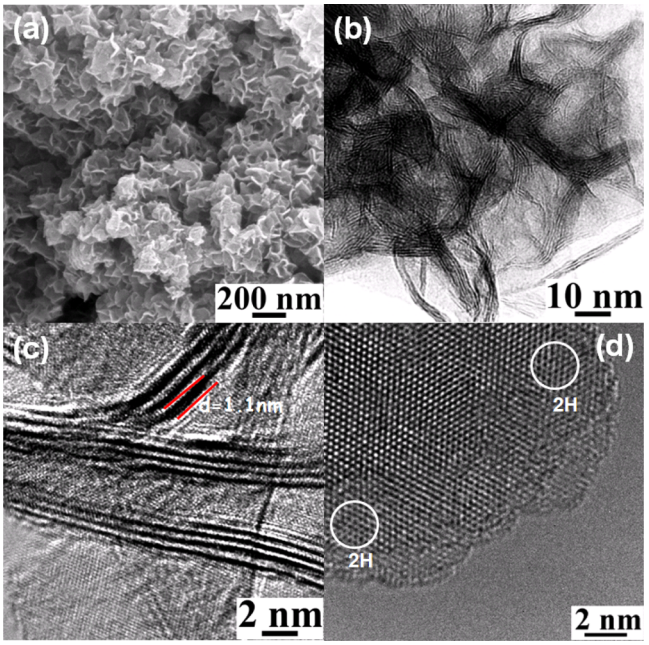

Figure 4. (a) SEM image, (b) low-magnification bright-field TEM image, and (c, d) HRTEM images of Co-doped MoS_2.

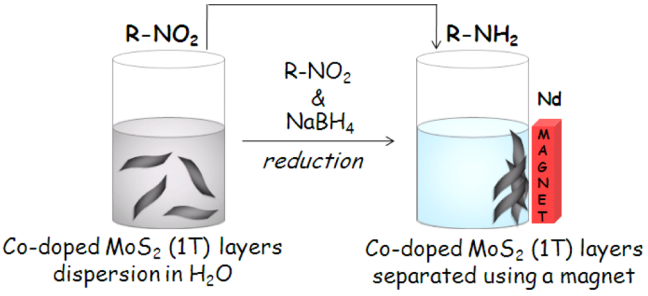

Figure 5. Schematic representation of the catalytic reduction of nitroarenes using Co-doped 1T MoS_2.

phenolate, and their intensities increase with time. The log (absorbance) versus time plot (Figure 6e) is linear (R^2 = 0.979), indicating a pseudo-first-order kinetics[47,48] with a rate constant of 1.976×10^{-3} s^{-1}. The turnover frequency (TOF) values, defined as the number of moles of the product formed per unit time per mole of the catalyst, of the materials studied are given in Table 2.

Apart from exhibiting a high TOF, the catalyst also has the advantage of recyclability. As the catalyst is weakly magnetic, it is easily separated from the reaction mixture using a strong magnet, enabling easy recycling (Figure 5). The catalytic activity of Co-doped MoS_2 remains nearly constant over a number of cycles (Figure 6f). The morphology and composition of the catalyst remain almost the same after six cycles of catalysis. Earlier attempts to make MoS_2-based catalysts magnetic have been through hybridization of MoS_2 nanosheets with magnetic nanoparticles such as Fe_3O_4.[27] One

DOI: 10.1021/acsomega.7b00848
ACS Omega 2017, 2, 5891–5897

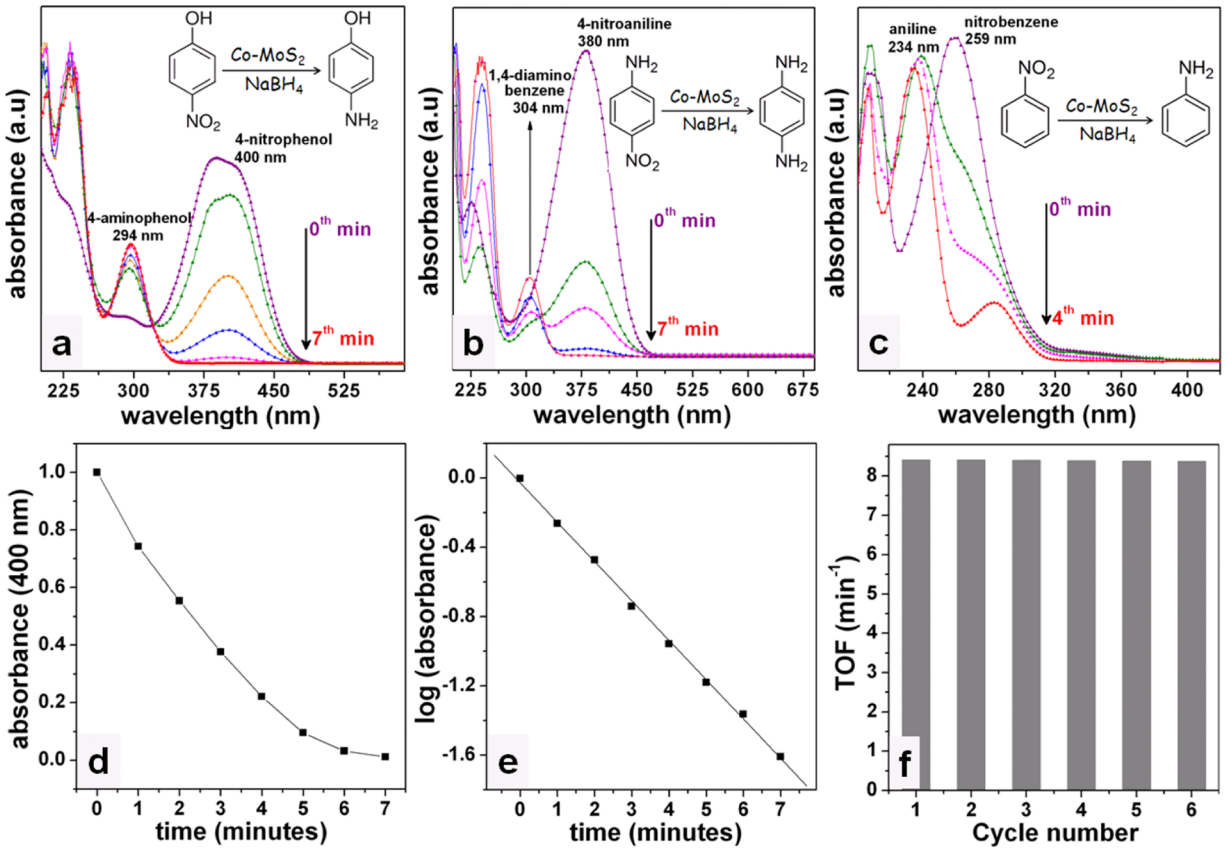

Figure 6. Reduction of nitroarenes was traced through UV−visible absorption spectra of the reaction mixture containing 10 mg of the Co-doped MoS_2 catalyst, 400 mM $NaBH_4$, and nitroarene. Evolution of absorption spectra with time in the case of 4-nitrophenol (a), 4-nitroaniline (b), and nitrobenzene (c). Plots of absorbance (d) and log (absorbance) (e) against time for 4-nitrophenol reduction. Efficiency of the catalyst (as TOF) in six consecutive cycles of 4-nitrophenol reduction (f).

Table 2. Catalytic Activity of the Catalysts in the Reduction of Nitroarenes

substrate	catalyst	time (min)	TOF (min^{-1})
4-nitrophenol (37 mM)	Co-doped MoS_2 (4.7% doping)	7	8.41
	Co-doped MoS_2 (~2% doping)	13.5	4.36
	Co-doped MoS_2 (~1% doping)	18	3.27
	acid-leached Co-doped MoS_2	8	7.36
	ammoniated MoS_2	90	0.65
4-nitroaniline (14 mM)	Co-doped MoS_2 (4.7% doping)	7	3.15
nitrobenzene (50 mM)	Co-doped MoS_2 (4.7% doping)	4	20.2

of the shortcomings of such approaches is the increased net weight of the catalyst because the magnetic component of the hybrid does not provide sites for catalytic action. Here, the advantage is that the dopant that improves the catalytic efficiency also makes the catalyst magnetic.

Treating Co-doped MoS_2 with an acid leads to deintercalation of interlayer NH_3/NH_4^+ and removal of about 30% of Co^{2+}, which were either intercalated or in the edge planes. Catalytic reduction of 4-NP using acid-leached Co-doped MoS_2 exhibits a slight decrease in catalytic activity (Table 2). In contrast, ammoniated 1T-MoS_2 synthesized in the absence of a cobalt source exhibits relatively very poor catalytic activity toward 4-NP reduction (Table 2). The comparison of the catalytic activities (Table 2) of the catalysts used in 4-NP reduction suggests that incorporation of cobalt ions in the MoS_2 lattice is crucial to maximizing the efficiency of the catalyst.

Figure 6b,c traces the reduction of nitroaniline and nitrobenzene, respectively, in the presence of as-prepared Co-doped MoS_2. The results show that the catalyst is universally effective in the reduction of nitro groups in different substrates and in at least two polar solvents. In fact, the catalyst is most efficient in the reduction of nitrobenzene, a reaction that is of importance in the removal of toxic nitrobenzene from effluents. In all of the cases, reduction of nitroarene does not occur in the absence of the catalyst.

In comparison to what has so far been reported in the literature (Table 3), the enhanced TOF and recyclability make Co-doped MoS_2 a superior catalyst. The TOF of Co-doped MoS_2 is 1 order greater than that of the best MoS_2-based catalyst and ~20% higher than the best value reported so far.

In Co-doped MoS_2, Co^{2+} takes residence at the coordinatively unsaturated sulfur vacancies on the basal plane and edge sites.[10,58] This leads to a conversion of a fraction of Mo^{4+} to Mo^{3+}, thus stabilizing the 1T polytype.[15] Doped Co^{2+} distorts the close-packed sulfur layer of MoS_2 and induces lattice strain.[59,60] These sites would lower the reaction free energy.[28] Nitroarenes are adsorbed at the strained active sites of the MoS_2 surface.[59−61] At these sites, the electron transfer to the substrate is facilitated by Co^{2+}/Co^{3+} redox couple. The electrons generated by the hydrolysis of $NaBH_4$ are transferred

DOI: 10.1021/acsomega.7b00848
ACS Omega 2017, 2, 5891−5897

Table 3. Comparison of TOF for the Reduction of Nitroarenes by Various Catalytic Materials Reported in the Literature

catalyst	TOF (min^{-1})	reference
4-nitrophenol reduction		
Co-doped MoS_2	8.41	present work
1T chemically exfoliated MoS_2	0.74	49
2H chemically exfoliated MoS_2	0.015	
MoS_2-Fe_3O_4	4.0×10^{-2}	27
MoS_2-Fe_3O_4/Pt	6.0×10^{-4}	50
MoS_2-Pd	3.2×10^{-3}	51
MoS_2-Pt		
MoS_2	2.5×10^{-3}	
MoS_2-Au		
MoS_2-Ag		
$Ni_{0.33}Co_{0.66}$	2.0×10^{-3}	52
citrate capped Au nanoparticles	1.4	53
Ag dendrites	0.13	54
Pd supported on CNTs	6.3	55
4-nitroaniline reduction		
Co-doped MoS_2	3.15	present work
1T chemically exfoliated MoS_2	1.39	49
Au nanowires	0.10	56
dodecahedral Au nanoparticles	0.10	57

to the Co^{2+}-accommodated basal and edge sites of 1T MoS_2 and are promoted into the MoS_2 conduction band.[59] The Co-substituted sites not only instigate faster electron transfer for nitroarene reduction through reversible reduction−oxidation reactions but also serve as an electron reserve and aid in the retention of the 1T phase with enhanced electrical conductivity.

The role of Co in improving the catalytic efficiency is very clear from the fact that the control MoS_2, which has intercalated NH_3/NH_4^+ and hence has similar access to surface as that of Co-doped MoS_2, shows poor activity (TOF is 1 order lower). As Co-doped MoS_2 is largely few-layer thick, the lattice expansion by intercalated species may not be very important and this is borne out from the almost similar activity of the acid-treated sample, which does not have intercalated species. This observation may be important when these catalysts are used in the hydrogen evolution reaction, the reaction medium of which is usually fairly acidic. To further ascertain the role of Co sites in catalysis, the catalytic activity of Co-doped MoS_2 with varying cobalt contents was studied. The increase in TOF of 4-nitrophenol reduction with an increase in Co doping (Table 2) further confirms the importance of Co sites in the catalyst.

3. CONCLUSIONS

Magnetic, 1T Co-doped MoS_2 nanosheets with the cobalt ion-activated defective basal planes and S-edges are synthesized in a single-step hydrothermal reaction. Readily dispersible in polar solvents like water or methanol, Co-doped MoS_2 nanosheets exhibit exceptional catalytic activity toward reduction of nitroarenes at ambient temperature. In addition to exhibiting a high turnover frequency, the catalyst can be magnetically separated from the reaction mixture, thus enabling recyclability simple and efficient. The superior catalytic activity of the Co-doped MoS_2 layers may be due to a combination of (a) stabilization of the metallic 1T phase and (b) better electron capture from the hydride and electron supply to the nitroarene substrates through reversible redox reactions at the Co sites.

4. EXPERIMENTAL SECTION

4.1. Preparation of Co-Doped MoS_2 Nanosheets. Cobalt acetate (0.214 g) was dissolved in 45 mL of water. Ammonium tetrathiomolybdate (0.442 g) was added to the pink Co^{2+} solution, and the mixture was stirred for 15 min. Hydrazine hydrate (5 mL) was added to the solution, and stirring was continued for another 15 min. The black-brown solution was transferred to a teflon-lined autoclave and sealed in a stainless steel canister. The autoclave was heated in a hot-air oven at 180 °C for 24 h and cooled to room temperature under ambient conditions. The pH of the supernatant at the end of the reaction was ∼12. The black precipitate was washed with distilled water till the pH of the washings is ∼7, followed by washing with acetone. The product was dried in air at ambient temperature. The preparation was repeated using 0.107 and 0.054 g of cobalt acetate to vary the cobalt content in the product.

4.2. Acid Leaching of Co-Doped MoS_2 Nanosheets. To extract the intercalated and free cobalt species, 100 mg of Co-doped MoS_2 was stirred in 5 mL of 1 N HCl for 24 h. The supernatant was collected. The process was repeated thrice. The cobalt content in the supernatant was estimated. The black solid was washed with water followed by acetone and dried in air at ambient temperature.

4.3. Preparation of MoS_2 Nanosheets. As a control experiment, the synthesis was repeated in the absence of cobalt acetate, which results in ammoniated MoS_2 nanosheets.

4.4. Reduction of Nitroarenes Using Co-Doped MoS_2 Nanosheets as a Catalyst. *4.4.1. Reduction of 4-Nitrophenol (4-NP).* The catalyst (10 mg) was dispersed in 100 mL of water by stirring for 1 h. 4-NP (512 mg, 37 mM) was dissolved in 100 mL of the catalytic dispersion. An excess of $NaBH_4$ (1.51 g, 400 mM) was added with constant stirring [4-NP:$NaBH_4$ molar ratio was 1:12]. The progress of the reaction was monitored by measuring the absorbance of 4-NP at 400 nm.

4.4.2. Reduction of 4-nitroaniline (4-NA). The catalyst (10 mg) was dispersed in 100 mL of water by stirring for 1 h. 4-NA (192 mg, 14 mM) was dissolved in 100 mL of the catalytic dispersion. An excess of $NaBH_4$ (1.51 g, 400 mM) was added with constant stirring [4-NA/$NaBH_4$ molar ratio was 1:28]. The progress of the reaction was monitored by measuring the absorbance of 4-NA at 380 nm.

4.4.3. Reduction of Nitrobenzene (NB). The catalyst (10 mg) was dispersed in 100 mL of methanol by stirring for 1 h. Nitrobenzene (0.52 mL, 50 mM) was dissolved in the dispersion. An excess of $NaBH_4$ (1.51 g, 400 mM) was added with constant stirring [NB/$NaBH_4$ molar ratio was 1:8]. The progress of the reaction was monitored by measuring the absorbance of nitrobenzene at 259 nm.

In all of the cases, an excess amount of $NaBH_4$ was used to ensure that its concentration could be considered constant throughout the reaction and the molar ratio in each case was optimized at the lowest $NaBH_4$ concentration that results in the shortest reaction time.

For comparison, the nitroarene reduction reactions were carried out (a) in the absence of the catalyst, (b) using control ammoniated MoS_2 nanosheets as a catalyst, and (c) acid-treated Co-MoS_2 nanosheets.

4.5. Characterization. All of the samples were analyzed by recording powder X-ray diffraction (XRD) patterns using a PANalytical X'pert pro diffractometer (Cu Kα radiation,

DOI: 10.1021/acsomega.7b00848
ACS Omega 2017, 2, 5891−5897

secondary graphite monochromator, scanning rate of 1° 2θ/min). The amount of Co^{2+} was estimated by a Varian AA240 atomic absorption spectrometer using a Co hallow cathode lamp in an air−acetylene flame at a wavelength of 324.4 nm. X-ray photoelectron spectroscopy (XPS) measurements were carried out with Kratos axis Ultra DLD. All spectra were calibrated to the binding energy of the C 1s peak at 284.51 eV. Scanning electron microscopy (SEM) analysis was carried out using a Zeiss, Ultra 55 field emission scanning electron microscope equipped with energy-dispersive X-ray spectroscopy (EDS). Transmission electron microscopy (TEM) images were acquired with Tecnai T20 operated at 200 kV. UV−visible spectra of the reaction mixtures were recorded on a PerkinElmer (LS 35) UV−visible spectrometer. The Raman spectra of the samples were recorded on HORIBA Jobin-Yvon LabRAM HR800 at 532 nm excitation wavelength. Isothermal magnetization [M vs H] was measured using a superconducting quantum interference device (SQUID) magnetometer.

■ ASSOCIATED CONTENT

Supporting Information

The Supporting Information is available free of charge on the ACS Publications website at DOI: 10.1021/acsomega.7b00848.

Raman spectrum of Co-doped MoS_2, and XPS data of acid leached Co-doped MoS_2 (PDF)

■ AUTHOR INFORMATION

Corresponding Author

*E-mail: mikerajamathi@rediffmail.com.

ORCID

Michael Rajamathi: 0000-0002-4975-1855

Notes

The authors declare no competing financial interest.

■ ACKNOWLEDGMENTS

This work was funded by SERB, India (EMR/2015/001982).

■ REFERENCES

(1) Chhowalla, M.; Shin, H. S.; Eda, G.; Li, L.-J.; Loh, K. P.; Zhang, H. The Chemistry of Two-Dimensional Layered Transition Metal Dichalcogenide Nanosheets. *Nat. Chem.* **2013**, *5*, 263−275.

(2) Hinnemann, B.; Moses, P. G.; Bonde, J.; Jørgensen, K. P.; Nielsen, J. H.; Horch, S.; Chorkendorff, I.; Nørskov, J. K. Biomimetic Hydrogen Evolution: MoS_2 Nanoparticles as Catalyst for Hydrogen Evolution. *J. Am. Chem. Soc.* **2005**, *127*, 5308−5309.

(3) Chia, X.; Eng, A. Y. S.; Ambrosi, A.; Tan, S. M.; Pumera, M. Electrochemistry of Nanostructured Layered Transition-Metal Dichalcogenides. *Chem. Rev.* **2015**, *115*, 11941−11966.

(4) Jaramillo, T. F.; Jørgensen, K. P.; Bonde, J.; Nielsen, J. H.; Horch, S.; Chorkendorff, I. Identification of Active Edge Sites for Electrochemical H_2 Evolution from MoS_2 Nanocatalysts. *Science* **2007**, *317*, 100−102.

(5) Prins, R.; De Beer, V. H. J.; Somorjai, G. A. Structure and Function of the Catalyst and The Promoter In Co−Mo Hydrodesulfurization Catalysts. *Catal. Rev.* **1989**, *31*, 1−41.

(6) Grange, P. Catalytic Hydrodesulfurization. *Catal. Rev.* **1980**, *21*, 135−181.

(7) Benck, J. D.; Chen, Z. B.; Kuritzky, L. Y.; Forman, A. J.; Jaramillo, T. F. Amorphous Molybdenum Sulfide Catalysts for Electrochemical Hydrogen Production: Insights Into The Origin of Their Catalytic Activity. *ACS Catal.* **2012**, *2*, 1916−1923.

(8) Merki, D.; Hu, X. L. Recent Developments of Molybdenum and Tungsten Sulfides As Hydrogen Evolution Catalysts. *Energy Environ. Sci.* **2011**, *4*, 3878−3888.

(9) Morales-Guio, C. G.; Hu, X. L. Amorphous Molybdenum Sulfides As Hydrogen Evolution Catalysts. *Acc. Chem. Res.* **2014**, *47*, 2671−2681.

(10) Bonde, J.; Moses, P. G.; Jaramillo, T. F.; Norskov, J. K.; Chorkendorff, I. Hydrogen Evolution on Nano-Particulate Transition Metal Sulfides. *Faraday Discuss.* **2012**, *5*, 219−231.

(11) Kibsgaard, J.; Chen, Z. B.; Reinecke, B. N.; Jaramillo, T. F. Engineering the Surface Structure of MoS_2 to Preferentially Expose Active Edge Sites for Electrocatalysis. *Nat. Mater.* **2012**, *11*, 963−969.

(12) Xie, J.; Zhang, H.; Li, S.; Wang, R.; Sun, X.; Zhou, M.; Zhou, J.; Lou, X. W.; Xie, Y. Defect-Rich MoS_2 Ultrathin Nanosheets with Additional Active Edge Sites for Enhanced Electrocatalytic Hydrogen Evolution. *Adv. Mater.* **2013**, *25*, 5807−5813.

(13) Xie, J.; Zhang, J.; Li, S.; Grote, F.; Zhang, X.; Zhang, H.; Wang, R.; Lei, Y.; Pan, B.; Xie, Y. Controllable Disorder Engineering in Oxygen-Incorporated MoS_2 Ultrathin Nanosheets for Efficient Hydrogen Evolution. *J. Am. Chem. Soc.* **2013**, *135*, 17881−17888.

(14) Kong, D.; Wang, H.; Cha, J. J.; Pasta, M.; Koski, K. J.; Yao, J.; Cui, Y. Synthesis of MoS_2 and $MoSe_2$ Films with Vertically Aligned Layers. *Nano Lett.* **2013**, *13*, 1341−1347.

(15) Wang, H.; Lu, Z.; Xu, S.; Kong, D.; Cha, J. J.; Zheng, G.; Hsu, P.-C.; Yan, K.; Bradshaw, D.; Prinz, F. B.; Cui, Y. Electrochemical Tuning of Vertically Aligned MoS_2 Nanofilms and Its Application In Improving Hydrogen Evolution Reaction. *Proc. Natl Acad. Sci. U.S.A.* **2013**, *110*, 19701−19706.

(16) Li, Y.; Wang, H.; Xie, L.; Liang, Y.; Hong, G.; Dai, H. MoS_2 Nanoparticles Grown on Graphene: An Advanced Catalyst for The Hydrogen Evolution Reaction. *J. Am. Chem. Soc.* **2011**, *133*, 7296−7299.

(17) Wang, H. T.; Lu, Z.; Kong, D.; Sun, J.; Hymel, T. M.; Cui, Y. Electrochemical Tuning of MoS_2 Nanoparticles on Three-Dimensional Substrate for Efficient Hydrogen Evolution. *ACS Nano* **2014**, *8*, 4940−4947.

(18) Jeffrey, A. A.; Rao, S. R.; Rajamathi, M. Preparation of MoS_2-Reduced Graphene Oxide (rGO) Hybrid Paper For Catalytic Applications by Simple Exfoliation-Costacking. *Carbon* **2017**, *112*, 8−16.

(19) Wang, F. Z.; Zheng, M. J.; Zhang, B.; Zhu, C. Q.; Li, Q.; Ma, L.; Shen, W. Z. Ammonia Intercalated Flower-like MoS_2 Nanosheet Film As Electrocatalyst For High Efficient and Stable Hydrogen Evolution. *Sci. Rep.* **2016**, *6*, No. 31092.

(20) Gao, M.-R.; Liang, J.-X.; Zheng, Y.-R.; Xu, Y.-F.; Jiang, J.; Gao, Q.; Li, J.; Yu, S.-H. An Efficient Molybdenum Disulfide/Cobalt Diselenide Hybrid Catalyst For Electrochemical Hydrogen Generation. *Nat. Commun.* **2015**, *6*, No. 5982.

(21) Huang, J.; Hou, D.; Zhou, Y.; Zhou, W.; Li, G.; Tang, Z.; Lia, L.; Chen, S. MoS_2 Nanosheet-Coated CoS_2 Nanowire Arrays on Carbon Cloth As Three-Dimensional Electrodes For Efficient Electrocatalytic Hydrogen Evolution. *J. Mater. Chem. A* **2015**, *3*, 22886−22891.

(22) Ranjith, B.; Jin, Z.; Shin, S.; Kim, S.; Lee, S.; Min, Y.-S. Co-catalytic Effects of CoS_2 on the Activity of the MoS_2 Catalyst for Electrochemical Hydrogen Evolution. *Langmuir* **2017**, *33*, 5628−5635.

(23) Wang, W.; Li, L.; Wu, K.; Zhu, G.; Tan, S.; Liu, Y.; Yang, Y. Highly Selective Catalytic Conversion of Phenols to Aromatic Hydrocarbons on CoS_2/MoS_2 Synthesized using a Two Step Hydrothermal Method. *RSC Adv.* **2016**, *6*, 31265−31271.

(24) Sorribes, I.; Liu, L.; Corma, A. Nanolayered Co-Mo-S Catalysts for Chemoselective Hydrogenation of Nitroarenes. *ACS Catal.* **2017**, *7*, 2698−2708.

(25) Yin, X.-L.; Li, L.-L.; Jiang, W. J.; Zhang, Y.; Zhang, X.; Wan, L.-J.; Hu, J.-S. MoS_2/CdS Nanosheets-on-Nanorod Heterostructure for Highly Efficient Photocatalytic H_2 Generation under Visible Light Irradiation. *ACS Appl. Mater. Interfaces* **2016**, *8*, 15258−15266.

(26) Liu, Y.; Yu, Y.-X.; Zhang, W.-D. MoS_2/CdS Heterojunction with High Photoelectrochemical Activity for H_2 Evolution under Visible Light: The Role of MoS_2. *J. Phys. Chem. C* **2013**, *117*, 12949−12957.

(27) Lin, T.; Wang, J.; Guo, L.; Fu, F. Fe_3O_4@MoS_2 Core−Shell Composites: Preparation, Characterization and Catalytic Application. *J. Phys. Chem. C* **2015**, *119*, 13658−13664.

DOI: 10.1021/acsomega.7b00848
ACS Omega 2017, 2, 5891−5897

(28) Voiry, D.; Yamaguchi, H.; Li, J.; Silva, R.; Alves, D. C. B.; Fujita, T.; Chen, M.; Asefa, T.; Shenoy, V. B.; Eda, G.; Chhowalla, M. Enhanced Catalytic Activity in Strained Chemically Exfoliated WS_2 Nanosheets for Hydrogen Evolution. *Nat. Mater.* **2013**, *12*, 850−855.
(29) Lukowski, M. A.; Daniel, A. S.; Meng, F.; Forticaux, A.; Li, L.; Jin, S. Enhanced Hydrogen Evolution Catalysis from Chemically Exfoliated Metallic MoS_2 Nanosheets. *J. Am. Chem. Soc.* **2013**, *135*, 10274−10277.
(30) Wang, Y.; Carey, B. J.; Zhang, W.; Chrimes, A. F.; Chen, L.; Kalantar-Zadeh, K.; Ou, J. Z.; Daeneke, T. Intercalated 2D MoS_2 Utilizing a Simulated Sun Assisted Process: Reducing the HER Overpotential. *J. Phys. Chem. C* **2016**, *120*, 2447−2455.
(31) Yan, Y.; Xia, Y. X.; Xu, Z.; Wang, X. Recent Development of Molybdenum Sulphides as Advanced Electrocatalysts For Hydrogen Evolution Reaction. *ACS Catal.* **2014**, *4*, 1693−1705.
(32) Merki, D.; Vrubel, H.; Rovelli, L.; Fierro, S.; Hu, X. L. Fe, Co, and Ni Ions Promote The Catalytic Activity of Amorphous Molybdenum Sulfide Films For Hydrogen Evolution. *Chem. Sci.* **2012**, *3*, 2515−2525.
(33) Wang, H.; Yuan, H.; Hong, S. S.; Li, Y.; Cui, Y. Physical and Chemical Tuning of Two-Dimensional Transition Metal Dichalcogenides. *Chem. Soc. Rev.* **2015**, *44*, 2664−2680.
(34) Liu, G.; Robertson, A. W.; Li, M. M.-J.; Kuo, W. C. H.; Darby, M. T.; Muhieddine, M. H.; Lin, Y.-C.; Suenaga, K.; Stamatakis, M.; Warner, J. H.; Tsang, S. C. E. MoS_2 Monolayer Catalyst Doped with Isolated Co Atoms For The Hydrodeoxygenation Reaction. *Nat. Chem.* **2017**, *9*, 810−816.
(35) Jeffery, A. A.; Nethravathi, C.; Rajamathi, M. Two-Dimensional Nanosheets and Layered Hybrids of MoS_2 and WS_2 through Exfoliation of Ammoniated MS_2 (M = Mo,W). *J. Phys. Chem. C* **2014**, *118*, 1386−1396.
(36) Dungey, K. E.; Curtis, M. D.; Penner-Hahn, J. E. Structural Characterization and Thermal Stability of MoS_2 Intercalation Compounds. *Chem. Mater.* **1998**, *10*, 2152−2161.
(37) Warren, B. E.; Bodenstein, P. The Diffraction Pattern of Fine Particle Carbon Blacks. *Acta Crystallogr.* **1965**, *18*, 282−286.
(38) Rajamathi, M.; Kamath, P. V.; Seshadri, R. Polymorphism in Nickel Hydroxide: Role of Interstratification. *J. Mater. Chem.* **2000**, *10*, 503−506.
(39) Ramakrishna Matte, H. S. S.; Gomathi, A.; Manna, A. K.; Late, D. J.; Datta, R.; Pati, S. K.; Rao, C. N. R. MoS_2 and WS_2 Analogues of Graphene. *Angew. Chem., Int. Ed.* **2010**, *49*, 4059−4062.
(40) Lee, C.; Yan, H.; Brus, L. E.; Heinz, T. F.; Hone, J.; Ryu, S. Anomalous Lattice Vibrations of Single- and Few-Layer MoS_2. *ACS Nano* **2010**, *4*, 2695−2700.
(41) Eda, G.; Yamaguchi, H.; Voiry, D.; Fujita, T.; Chen, M.; Chhowalla, M. Photoluminescence from Chemically Exfoliated MoS_2. *Nano Lett.* **2011**, *11*, 5111−5116.
(42) Yan, Y.; Xia, B. Y.; Ge, X.; Liu, Z.; Wang, J.-Y.; Wang, X. Ultrathin MoS_2 Nanoplates With Rich Active Sites As Highly Efficient Catalyst For Hydrogen Evolution. *ACS Appl. Mater. Interfaces* **2013**, *5*, 12794−12798.
(43) Luxa, J.; Jankovsky, O.; Sedmidubsky, D.; Medlin, R.; Marysko, M.; Pumera, M.; Sofer, Z. Origin of Exotic Ferromagnetic Metal Dichalcogenides MoS_2 and WS_2. *Nanoscale* **2016**, *8*, 1960−67.
(44) Wang, Y.; Li, S.; Yi, J. Electronic and Magnetic Properties of Co Doped MoS_2 Monolayer. *Sci. Rep.* **2017**, *6*, No. 24153.
(45) Yun, W. S.; Lee, J. D. Strain-Induced Magnetism in Single-Layer MoS_2: Origin and Manipulation. *J. Phys. Chem. C* **2015**, *119*, 2822−2827.
(46) Saab, M.; Raybaud, P. Tuning the Magnetic Properties of MoS_2 Single Nanolayers by 3d Metals Edge Doping. *J. Phys. Chem. C* **2016**, *120*, 10691−10697.
(47) Gu, X.; Qi, W.; Xu, X.; Sun, Z.; Zhang, L.; Liu, W.; Pan, X.; Su, D. Covalently functionalized carbon nanotube supported Pd nanoparticles for catalytic reduction of 4-nitrophenol. *Nanoscale* **2014**, *6*, 6609−6616.
(48) Huang, J.; Zhu, Y.; Lin, M.; Wang, Q.; Zhao, L.; Yang, Y.; Yao, K. X.; Han, Y. Site-Specific Growth of Au−Pd Alloy Horns on Au Nanorods: A Platform for Highly Sensitive Monitoring of Catalytic Reactions by Surface Enhancement Raman Spectroscopy. *J. Am. Chem. Soc.* **2013**, *135*, 8552−8561.
(49) Guardia, L.; Paredes, J. I.; Munuera, J. M.; Rodil, S. V.; Ayan-Varela, M.; Martinez-Alonso, A.; Tascón, J. M. D. Chemically Exfoliated MoS_2 Nanosheets as an Efficient Catalyst for Reduction Reactions in the Aqueous Phase. *ACS Appl. Mater. Interfaces* **2014**, *6*, 21702−21710.
(50) Cheng, Z.; He, B.; Zhou, L. A general one-step approach for in situ decoration of MoS_2 nanosheets with inorganic nanoparticles. *J. Mater. Chem. A* **2015**, *3*, 1042−1048.
(51) Qiao, X.-Q.; Zhang, Z.-W.; Tian, F.-Y.; Hou, D.-F.; Tian, Z.-F.; Li, D.; Zhang, Q. Enhanced catalytic reduction of p-nitrophenol on ultrathin MoS_2 nanosheets decorated noble-metal nanoparticles. *Cryst. Growth Des.* **2017**, *17*, 3538−3547.
(52) Wu, K.-L.; Wei, X.-W.; Zhou, X.-M.; Wu, D.-H.; Liu, X.-W.; Ye, Y.; Wang, Q. $NiCo_2$ Alloys: Controllable Synthesis, Magnetic Properties, and Catalytic Applications in Reduction of 4-Nitrophenol. *J. Phys. Chem. C* **2011**, *115*, 16268−16274.
(53) He, R.; Wang, Y. C.; Wang, X.; Wang, Z.; Liu, G.; Zhou, W.; Wen, L.; Li, Q.; Wang, X.; Chen, X.; Zeng, J.; Hou, J. G. Facile synthesis of pentacle gold−copper alloy nanocrystals and their plasmonic and catalytic properties. *Nat. Commun.* **2014**, *5*, No. 4327.
(54) Rashid, Md. H.; Mandal, T. K. Synthesis and Catalytic Application of Nanostructured Silver Dendrites. *J. Phys. Chem. C* **2007**, *111*, 16750−16760.
(55) Li, H.; Han, L.; Cooper-White, J.; Kim, I. Palladium nanoparticles decorated carbon nanotubes: facile synthesis and their applications as highly efficient catalysts for the reduction of 4-nitrophenol. *Green Chem.* **2012**, *14*, 586−591.
(56) Chirea, M.; Freitas, A.; Vasile, B. S.; Ghitulica, C.; Pereira, C. M.; Silva, F. Gold Nanowire Networks: Synthesis, Characterization, and Catalytic Activity. *Langmuir* **2011**, *27*, 3906−3913.
(57) Chiu, C.-Y.; Chung, P.-J.; Lao, K.-U.; Liao, C.-W.; Huang, M. H. Facet-Dependent Catalytic Activity of Gold Nanocubes, Octahedra, and Rhombic Dodecahedra toward 4-Nitroaniline Reduction. *J. Phys. Chem. C* **2012**, *116*, 23757−23763.
(58) Clausen, B. S.; Topsoe, H.; Candia, R.; Villadsen, J.; Lengeler, B.; Als-Nielsen, J.; Christensen, F. Extended X-ray Absorption Fine Structure Study of the Cobalt-Molybdenum Hydrodesulfurization Catalysts. *J. Phys. Chem.* **1981**, *85*, 3868−3872.
(59) Brenner, J.; Marshall, C. L.; Ellis, L.; Tomczyk, N.; Heising, J.; Kanatzidis, M. Microstructural Characterization of Highly HDS-Active Co_6S_8-Pillared Molybdenum Sulfides. *Chem. Mater.* **1998**, *10*, 1244−1257.
(60) Chianelli, R. R.; Ruppert, A. F.; José-Yacamán, M.; Vázquez-Zavala, A. HREM Studies of Layered Transition Metal Sulphides Catalytic Materials. *Catal. Today* **1995**, *23*, 269−281.
(61) Li, H.; Chen, S.; Jia, X.; Xu, B.; Lin, H.; Yang, H.; Song, L.; Wang, X. Amorphous nickel-cobalt complexes hybridized with 1T-phase molybdenum disulfide via hydrazine-induced phase transformation for water splitting. *Nat. Commun.* **2017**, *8*, No. 15377.

DOI: 10.1021/acsomega.7b00848
ACS Omega 2017, 2, 5891−5897